Organic Process Research & Development **2009,** *13,* 941–951

Full Papers

Design and Performance of a Microstructured PEEK Reactor for Continuous Poly-L-leucine-Catalysed Chalcone Epoxidation

Suet-Ping Kee and Asterios Gavriilidis*

Department of Chemical Engineering, University College London, Torrington Place, London WC1E 7JE, U.K.

Abstract:

The poly-L-leucine (PLL)-catalysed epoxidation of chalcone allows access to highly enantioselective chalcone epoxides. The reaction requires two steps, a deprotonation step where the oxidising reactive species is formed and an epoxidation step where the substrate is epoxidised. In this work, a microstructured SU-8/PEEK plate flow reactor with a footprint of 110 mm × 85 mm and production rate of ~0.5 g/day was designed. The reactor consists of two micromixer−reactor sections in series. A staggered herringbone micromixer design was employed for efficient mixing, with channel width, height, and length of 0.2, 0.085, and 40 mm respectively. A mathematical model was used to aid the design, and its predictions were compared with experimental results. The deprotonation and epoxidation steps were performed in reaction channels with width and height of 2 and 0.33 mm, while lengths of 450 and 480 mm provided residence times for the two steps of 30 and 16 min, respectively. The effects of operating temperature, reactant and catalyst concentrations, and residence time on reaction performance were investigated. The base case condition (13.47 g/L PLL, 0.132 mol/L H_2O_2, 0.0802 mol/L chalcone, 0.22 mol/L DBU) was found to be optimal, achieving a conversion of 86.7% and enantioselectivity of 87.6%. Comparison between model and experimental results provided insight into the reaction mechanism as well as reactor design. It showed quantitative and, in some cases, qualitative differences. These were attributed to the simplicity of the kinetic model, bubble formation from peroxide decomposition and their stagnation in the rectangular channels, and high viscosity of catalyst solution which may have affected mixing performance.

Introduction

The need for more efficient process development and manufacturing methods, as well as the general shift towards inherently safer and greener processes has led pharmaceutical companies to increasingly re-evaluate the use of continuous processing and look into using innovative technologies as an alternative to conventional batch processes.[1−3] The pharmaceuticals and fine chemicals industry have traditionally relied heavily on batch reactors, which are flexible towards frequent product changes and production rates and can accommodate various downstream operations. Flexibility and versatility of the equipment is required, given the relatively low volumes and short lifetime of the products, to limit the investment costs.

On the other hand, continuous processing is generally preferred in the commodity chemicals sector because it is operationally stable and offers better process control, consistent product quality, enhanced safety, lower operating costs, and it allows more material to be made from a smaller plant. However, continuous processing relies on dedicated processing plants that are inflexible and not amenable to varying production rates or product changes.[1]

Recent technological advances in the field of microreaction technology offer the opportunity to combine the benefits of continuous processing with the flexibility and versatility desired in the pharmaceutical and fine chemicals industry.[2,4] Microreactor devices, generally defined as miniaturised reaction systems fabricated by microtechnology and precision engineering, offer unique advantages over traditional continuous processing. The high surface to volume ratios allow for highly efficient heat and mass transfer, while small reaction volumes allow safer handling of exothermic reactions and easy containment of explosive and toxic materials. These characteristics allow precise control of reaction parameters and access to new reaction regimes that could potentially improve yield and selectivity, making the process more efficient and cost-effective. Production rates in microreactors can be increased by scaling out (i.e., increasing the number of reactor units) rather than scaling up (i.e., increasing the size of the reactor), to supply increasing amounts of material for clinical trials as the drug progresses through the regulatory process. Scaling out is promising as the process optimization from laboratory to pilot scales can be bypassed, allowing for significant savings on time and R&D costs. In this work, a microchannel reactor, amenable to scale-out, is designed and evaluated for chalcone epoxidation.

Reactor Design Considerations

Poly-L-leucine-Catalysed Asymmetric Epoxidation of Chalcone. The poly-L-leucine (PLL)-catalysed asymmetric epoxidation of chalcone allows highly enantioselective synthesis

* Corresponding author. Telephone: +44 (0)20 7679 3811. Fax: +44 (0)20 73832348. E-mail: a.gavriilidis@ucl.ac.uk.

(1) Anderson, N. G. *Org. Process Res. Dev.* **2001**, *5*, 613.
(2) Schwalbe, T.; Autze, V.; Hohmann, M.; Stirner, W. *Org. Process Res. Dev.* **2004**, *8*, 440.
(3) Stitt, E. H. *Chem. Eng. J.* **2002**, *90*, 47.
(4) Roberge, D. M.; Ducry, L.; Bieler, N.; Cretton, P.; Zimmermann, B. *Chem. Eng. Technol.* **2005**, *28*, 318.

10.1021/op800276a CCC: $40.75
Published on Web 04/27/2009

of chiral epoxides, which are useful intermediates for the synthesis of active ingredients and hence represent a commercially important synthesis for the pharmaceutical industry. Chalcone is epoxidised to (2*R*,3*S*)-chalcone epoxide, in the presence of polyethylene glycol-poly-L-leucine (PLL) as catalyst, hydrogen peroxide extracted from urea−hydrogen peroxide adducts as oxidant and 1,8-diazabicyclo[5.4.0]undec-7-ene (DBU) as base. The solvent is mixed tetrahydrofuran (THF) and acetonitrile (ACN), with a THF:ACN ratio of 2.15.

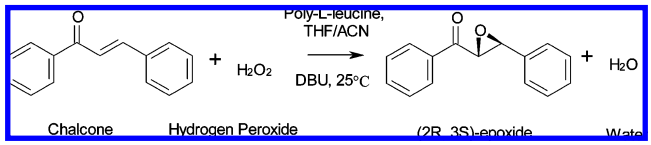

The first step of the reaction involves a prereaction equilibria (deprotonation). The reactive peroxy anion species is formed from the peroxide by addition of the base. The peroxy anion adsorbs on the catalyst and in the second step (epoxidation) reacts with chalcone to provide the epoxide. The competing background epoxidation occurs in the absence of catalyst, with chalcone epoxidised to both (2*R*,3*S*)-chalcone epoxide and (2*S*,3*R*)-chalcone epoxide, resulting in a racemic product.

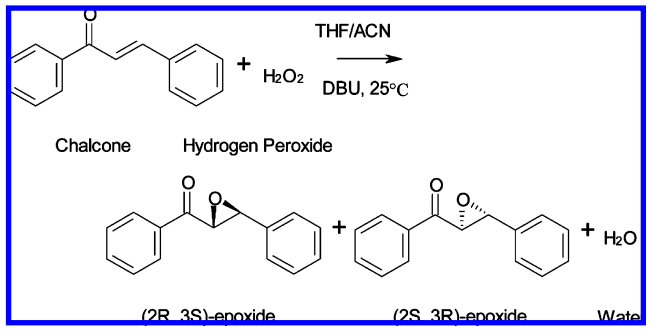

The ranges of reactant concentrations used in the kinetic study to derive the rate equations[5] were PLL: 7.94−22.96 g/L, chalcone: 0.014−0.1788 mol/L, peroxide: 0.034−0.14 mol/L. The average heat of reaction was found to be −111 kJ/mol. The rate equations for both the main and competing reactions at 23.1 °C are shown in eqs 1 and 2, with values of the kinetic constants: $k = 2.38 \times 10^{-3}$ L^2/g•mol•s, $K_{Chalcone} = 2.172$ L/mol, $K_{H_2O_2} = 1.092$ L/mol, $k_{BG} = 2.2 \times 10^{-3}$ L/mol•s.[5]

$$\mathrm{Rate}_{PLL-Catalysed} = \frac{k[\mathrm{Cat}][\mathrm{Chalcone}][H_2O_2]}{(1 + K_{Chalcone}[\mathrm{Chalcone}] + K_{H_2O_2}[H_2O_2])} \quad (1)$$

$$\mathrm{Rate}_{Background} = k_{BG}[\mathrm{Chalcone}][H_2O_2] \quad (2)$$

Design Basis. In our previous work,[6] the initial batch process was improved to prevent formation of precipitates and allow the reaction to be transferred to a continuous flow process. Following that, a continuous reaction protocol was established, and several design issues were identified. On the basis of these findings, a continuous setup comprising two micromixers and two tubular reactors for the deprotonation and epoxidation steps was employed for milligram-scale synthesis. In this work, the objective is to design a continuous flow system for gram-scale production. An integrated planar format is adopted, so that the reactor system will be amenable to scale-out. As diffusional mixing was previously found to be slow due to the low diffusivity of PLL, methods for enhancing mixing were considered. The reaction channel was sized to provide sufficient residence time and ensure a tight residence time distribution. Heat management was less crucial in this case, due to the low adiabatic temperature rise.

Mixing Considerations. The simplest micromixer is the T-micromixer where two streams are combined at a T-junction and sufficient residence time is provided downstream of the junction for complete mixing. Mixing typically occurs by molecular diffusion only; depending on the diffusivity of the reactants and the rate of reaction, this may be acceptable. However, for reactants with very low diffusivity values or with very fast reactions, the rate of mixing in a T-micromixer may not be acceptable and needs to be enhanced. Several methods have been shown to enhance mixing for continuous reaction systems[7−10] including interdigital multilamination, split and recombine, geometric focussing, and chaotic mixing methods.

As a first step in selecting a suitable mixing device, the required diffusional mixing times in a T-mixer with a characteristic diffusion length of 100 μm were calculated for both chalcone and PLL. For chalcone and PLL with typical molecular diffusivities of 10^{-9} and 10^{-11} m^2/s, respectively, the diffusional mixing times were $t_{Chalcone} = L_{dif}^2/D = 10$ s, $t_{PLL} = 1000$ s. The reaction time constants were considered as the half-time of the reactions. In chalcone epoxidation, two reactions occur: (a) the poly-L-leucine-catalysed reaction, (b) the background reaction. The initial concentrations of chalcone and peroxide are $C_{A0} = 0.0802$ mol/L and $C_{B0} = 0.132$ mol/L respectively. Assuming $C_{A0} = C_{B0} = 0.132$ mol/L, we obtain reaction time constants of 5.1 and 57 min for the catalysed and the background reactions, respectively. This shows that the catalysed reaction is much faster than the background reaction. The ratio of diffusional mixing time to reaction time constants for catalysed and background reactions are: $\mathrm{Diffusion}_{PLL}/\mathrm{Rate}_{PPL\text{-}catalysed} = 3.26$, $\mathrm{Diffusion}_{Chalcone}/\mathrm{Rate}_{Background} = 0.00292$. Hence, at a diffusion length scale of 100 μm, the diffusion process is slower than the catalysed reaction.

For minimal influence of mixing on reaction, the diffusion time should be significantly smaller than the catalysed reaction time. At a ratio of diffusion to reaction time constants of 0.01, the diffusion time required would be 3.1 s, which corresponds to a characteristic length of 5.5 μm. This is clearly not practical with a simple T-micromixer; at such low dimensions, the system is prone to clogging. This means that simple mixing by diffusion is insufficient and needs to be enhanced by other methods. Of the various methods for enhancing mixing,[7−10] the staggered

(5) Mathew, S. Internal Project Report: *Kinetics of epoxidation of chalcone to chalcone epoxide using soluble poly-L-leucine catalyst*; University of Hull: Hull, U.K., 2003.

(6) Kee, S. P.; Gavriilidis, A. *J. Mol. Catal A: Chem.* **2007**, *263*, 156.
(7) Ehrfeld, W., Hessel, V., Löwe, H. *Microreactors: New Technology for Modern Chemistry*: Wiley-VCH: Weinheim, 2000.
(8) Jiang, F.; Drese, K. S.; Hardt, S.; Kupper, M.; Schönfeld, F. *AIChE J.* **2004**, *50*, 2297.
(9) Schönfeld, F.; Hessel, V.; Hofmann, C. *Lab Chip* **2004**, *4*, 65.
(10) Stroock, A. D.; Dertinger, S. K. W.; Ajdari, A.; Mezic, I.; Stone, H. A.; Whitesides, G. M. *Science* **2002**, *295*, 647.

Table 1. **Details of staggered herringbone mixer design used in PEEK reactor**

design parameter	value
channel width, w (μm)	200
channel height, h (μm)	85
groove depth, $2\alpha h$ (μm)	31
groove period, $2\pi/q$ (μm)	100
angle, θ (deg)	45
grooves/half-cycle	6
length per cycle (mm)	1.516
number of cycles	26
total mixer length (mm)	40

herringbone mixer was chosen as it offers both ease of fabrication and mixing efficiency. The mixing length and time required was estimated on the basis of the work of Stroock et al.[10] It was found that at the selected channel dimensions and flow conditions, the mixing length required is ~0.9 cm with corresponding mixing time of 0.5 s. To allow sufficient margin for ensuring complete mixing and flexibility for higher flows, a mixer length of 4 cm was used. All the mixer design parameters are given in Table 1.

Reactor Design Considerations. In a tubular reactor, for plug flow to be applicable, the following criteria must be met:[11]

$$\frac{d}{L} \ll Re_d Sc \ll \frac{L}{d}, \quad \text{where } Re_d Sc = \frac{\rho u d}{\mu}\frac{\mu}{\rho D_n} = \frac{ud}{D_n} \tag{3}$$

The lower bound ensures that the axial diffusive transport over the length scale L is negligible compared to axial convective transport, while the upper bound ensures that there are no radial variations. Rearranging eq 3 we get

$$Pe_r = \frac{ud^2}{D_n L} \ll 1 \tag{4}$$

for negligible radial concentration gradients

$$Pe_z = \frac{uL}{D_n} \gg 1 \tag{5}$$

for negligible axial diffusive transport.

For a wide-slit reactor, d is replaced by $2Y$, the height of the slit and the Pe_r becomes:

$$Pe_r = \frac{uY^2}{D_n L} = \frac{Y^2}{D_n \tau} \ll 0.25 \tag{6}$$

Mathematical Model. A slit laminar flow reactor model was set up to investigate the effect of reactor geometry on reaction performance for design purposes. The deprotonation reaction was not taken into account since the rate equation was not available; however, provided sufficient residence time was available, the final concentration of the peroxy anion should be the same (at base case conditions). The required residence time for the deprotonation reaction was established experimentally in our previous work. The axial velocity profile for laminar, Newtonian fluid of constant viscosity in a slit is given by:

$$V_z(y) = 1.5\bar{u}\left(1 - \frac{y^2}{Y^2}\right) \tag{7}$$

The material balance in a slit laminar flow reactor at steady-state conditions is given by eq 8. The change in concentration of each component due to reaction, $\mathscr{R}_n$, is calculated based on the catalysed and background reaction stoichiometries and reaction rates.

$$V_z(y)\frac{\partial C_n}{\partial z} = D_n\left[\frac{\partial^2 C_n}{\partial z^2} + \frac{\partial^2 C_n}{\partial y^2}\right] + \mathscr{R}_n \tag{8}$$

For a reactor with height $2Y$ and length L, the two independent variables z and y can be scaled with length L and half-height Y, respectively. Substituting the new variables ($\xi = z/L$, $\zeta = y/Y$) and eq 7 into eq 8 we get:

$$1.5(1 - \zeta^2)\frac{\partial C_n}{\partial \xi} = \left(\frac{D_n\tau}{Y^2}\right)\left[\left(\frac{Y^2}{L^2}\right)\frac{\partial^2 C_n}{\partial \xi^2} + \frac{\partial^2 C_n}{\partial \zeta^2}\right] + \mathscr{R}_n\tau \tag{9}$$

where $((D_n\tau)/(Y^2))$ can be taken as Pe_r^{-1}. Heat transfer is governed by similar equations; the energy balance is given in eq 10. This equation assumes constant thermal diffusivity, α_T, and density, ρ.

$$1.5(1 - \zeta^2)\frac{\partial T}{\partial \xi} = \left(\frac{\alpha_T\tau}{Y^2}\right)\left[\left(\frac{Y^2}{L^2}\right)\frac{\partial^2 T}{\partial \xi^2} + \frac{\partial^2 T}{\partial \zeta^2}\right] + \frac{H_{Rxn}\mathscr{R}_n\tau}{\rho C_p} \tag{10}$$

where $\alpha_T = \lambda/(\rho C_p)$.

The boundary conditions used are as follows:

(1) Across the entire cross section, $\zeta = 0-1$

At the inlet, $\xi = 0$,

$$C_n(0,\zeta) = C_{n0} \tag{11a}$$

$$T(0,\zeta) = T_0 \tag{11b}$$

At the outlet, $\xi = 1$

$$\frac{\partial C_n}{\partial \xi} = 0, \quad \frac{\partial T}{\partial \xi} = 0 \tag{12}$$

(2) Across the entire reactor length $\xi = 0-1$

At $\zeta = 0$

$$\frac{\partial C_n}{\partial \zeta} = 0, \quad \frac{\partial T}{\partial \zeta} = 0 \tag{13}$$

At the wall, $\zeta = 1$

$$\frac{\partial C_n}{\partial \zeta} = 0, \quad T = T_{wall} \tag{14}$$

The inside wall temperature was assumed to be equal to the outside wall temperature. Conversion, X, and enantioselectivity, S, values were computed from eqs 15 and 16 using mixing cup average outlet concentrations computed from eq 17.

(11) Raja, L. L.; Kee, R. J.; Deutschmann, O.; Warnatz, J.; Schmidt, L. D. *Catal. Today* **2000**, *59*, 47.

$$X = \frac{C_{\text{Chalcone},\tau=0} - C_{\text{Chalcone},\tau}}{C_{\text{Chalcone},\tau=0}} \quad (15)$$

$$S = \frac{C_{\text{Product},\tau} - C_{\text{Byproduct},\tau}}{C_{\text{Product},\tau} + C_{\text{Byproduct},\tau}} \quad (16)$$

$$C_{n,\text{mix}} = 1.5 \int_0^1 C_n(\zeta, \xi)[1 - \zeta^2]\mathrm{d}\zeta \quad (17)$$

The model was solved using gPROMS on Windows XP with Pentium IV 3.00 GHz CPU and 512 MB of RAM. The axial domain was discretized using centered finite differences (CFDM) of second order over a uniform grid of 150 intervals, while second-order orthogonal collocation (OCFEM) over 20 finite elements was adopted for the transverse direction. Increasing the number of intervals to 300 or the number of finite elements to 40 did not change the results.

Sizing of Reactor Channel. Given the relatively long residence time required, there is a trade-off between maximising the effects of diffusion (reduce Y to facilitate transverse mass transfer, which increases the total length) and minimising the footprint of the reactor (reduce total length). The epoxidation channel was sized to allow for 16 min residence time at a total volume of 0.32 mL. The reaction channels were dimensioned to fulfill eqs 5 and 6, as well as $Y/w < 0.1$ to ensure negligible side-wall effects. For a rectangular channel, the pressure drop can be calculated from:

$$\Delta P = \frac{128\mu LQ}{\pi D_{\text{E}}^4} \quad (18)$$

where Q and L represent the volumetric flow rate and channel length. D_{E}, the equivalent diameter for a rectangular channel with width w and height h, can be calculated from:

$$D_{\text{E}} = \left(\frac{128wh^3}{\pi K}\right)^{1/4} \quad (19)$$

where K is a constant, the value of which depends on the ratio w/h.[12] The channel length required at channel widths 0.5−3 mm and heights 0.08−0.5 mm, was found to be in the range 200−8000 mm, with pressure drop in the range 10^{-1}−10^5 Pa. Shallow channels allow for high values of Pe_{r}^{-1} but result in excessively long reaction channels. The length can be reduced by increasing the channel width. However, a channel that is too wide requires larger footprint and may result in unnecessary dead volumes. Narrow channels are also preferred as they minimise the expansion from a mixer width of 200 μm. In this case, the selection of the reactor channel dimensions was driven mainly by the decision to adhere to a maximum footprint of 85 mm × 110 mm. The effect of several different values of Pe_{r}^{-1} at channel width of 2 mm on the conversion was investigated using the model. Conversion improved with increasing Pe_{r}^{-1} up to $Pe_{\text{r}}^{-1} = 2$, beyond which improvement was only marginal. For this reason, the 2 mm wide channel was selected even though Pe_{r}^{-1} was below 4, as it allows for a reasonable reactor length to be used. The selected dimensions for both the deprotonation and epoxidation channels are shown in Table 2.

Table 2. **Reaction channel dimensions**

	deprotonation	epoxidation
channel width (μm)	2000	2000
channel height (μm)	330	330
channel length (mm)	450	480
$1/Pe_{\text{r}}$	5	3
residence time (min)	30	16

Heat Transfer Considerations. The reaction is not highly exothermic; the heat of reaction of −111 kJ/mol results in an adiabatic temperature rise of 4.9 K. Moreover, if the inside reactor wall temperature is maintained at the required design temperature, the change in temperature is found to be negligible (<0.002 K). This is achieved by placing the reactor in a water bath at the required temperature. The inside wall temperature was assumed to be equal to the outside wall temperature due to the thin walls and the low adiabatic temperature rise. A CFD simulation (with COMSOL) was carried out to ensure that sufficient length is provided for the entering fluids to be heated/cooled prior to contacting. It was found that the inlet fluids reached the desired temperature within a very short distance (<0.3 mm) at both 0.005 mL/min (first micromixer) and 0.01 mL/min (second micromixer).

Experimental Details

Reactor Fabrication. Advances in microfabrication techniques mean that microdevices are no longer confined to silicon and are now available in glass, stainless steel, ceramics, polymers such as polymethyl methacrylate, Mylar, polycarbonate, polydimethylsiloxane, cyclo-olefin copolymer, and polyethylene terephthalate. A review on the potential applications of plastics and polymers as substrate materials in microfluidic applications is available.[13] The reaction conditions for chalcone epoxidation can be quite harsh due to the choice of reaction solvents such as THF and ACN, which are incompatible with various materials. The basic conditions, due to the presence of the organic base DBU, further aggravates the situation. The choice of material of construction should ideally fulfill the following criteria: (a) relatively low cost, (b) appropriate chemical compatibility, (c) good optical properties, (d) easily machinable and applicable to mass replication technologies, (e) facile bonding of the structured plates. While for production purposes, a robust material such as stainless steel is generally preferred, microstructured stainless steel can be expensive. Similarly, fabrication costs for glass, which is inert and has good optical properties, are also high. Acrylic (polymethyl methacrylate) has good optical properties and is relatively inexpensive to fabricate but is not chemically compatible with THF and ACN. Polyetheretherketone (PEEK) which is chemically compatible with THF and ACN below 70 °C was selected, as it is relatively inexpensive and is amenable to mass replication. A similar design was also fabricated in acrylic for flow visualisation purposes.

Both the PEEK and acrylic reactors were fabricated by Epigem Ltd. (UK) using photolithographic methods for micro-

(12) Perry, R. H., Green, D. W. *Perry's Chemical Engineers' Handbook*, 7th ed.; McGraw-Hill: New York, 1997.

(13) de Mello, A. *Lab Chip* **2002**, *2*, 31N.

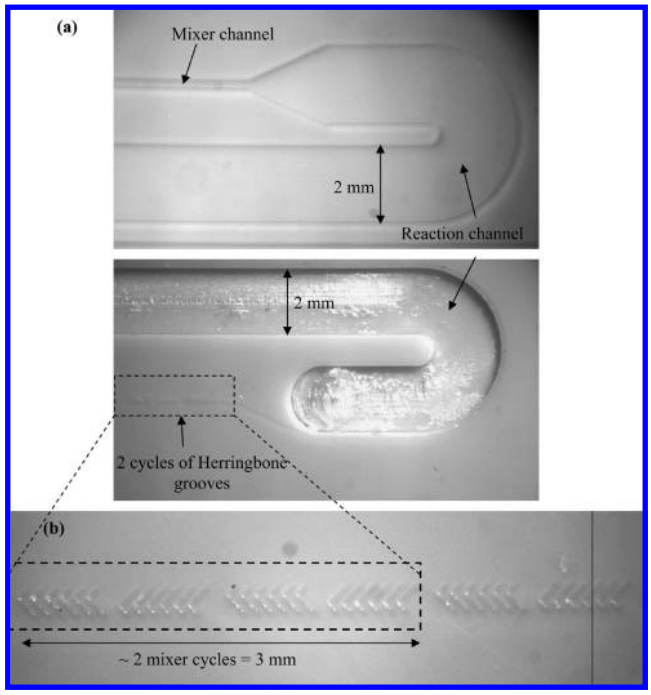

Figure 1. **Microscope photographs of unbonded PEEK reactor. (a) Matching PEEK plates which form the reactor after bonding. (b) Herringbone grooves etched on SU-8.**

structures (<150 μm deep and 300 μm wide) and machining methods for larger mili-scale structures. SU-8, an epoxy-based negative photoresist, has gained popularity for fabrication of microfluidics components due to its superior chemical and mechanical properties and ease of fabrication.[14] The fabrication process uses an SU-8 layer spin-coated on a thin plate (which can be PEEK or acrylic), where the microstructures are patterned on the SU-8 layer and are therefore completely surrounded by SU-8. The mili-scale structures, on the other hand consist of both plate material and SU-8. The reactors are bonded via diffusion bonding using SU-8. For the PEEK microstructured reactor design, channel depths of 85 μm for both mixer and reactor channels were etched onto one plate, while the herringbone grooves and reactor channel depth of 245 μm were etched/machined onto another plate. The two plates were then aligned and bonded together to give a channel depth of 85 μm in the micromixer section and 330 μm in the reaction channel section. Photographs of the two sides, focusing on the section where the micromixers expand to the reaction channel entrance, are shown in Figure 1. Figure 2 shows the assembled reactor in both PEEK and acrylic.

Experimental Setup and Procedures. An XP 3000 Modular Digital Pump (Cavro) with three 50-μL syringes was used to pump solutions of chalcone, DBU and catalyst/peroxide. Three solutions were prepared: a 0.16 mol/L chalcone solution, a 0.88 mol/L DBU solution and a PLL/peroxide solution of 53.88 g/L PLL and 0.53 mol/L peroxide. Three inline 2 μm stainless steel filters were connected to all three reactant inlets to prevent clogging. DBU and PLL/peroxide solutions were pumped at a flow rate of 5 μL/min each, to the first staggered herringbone mixer followed by a 0.3 mL delay loop with 30

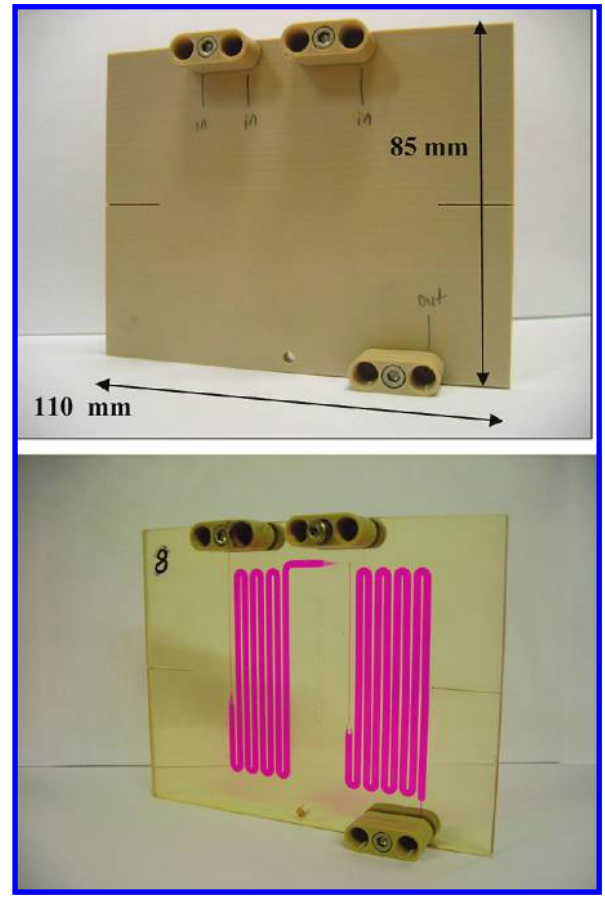

Figure 2. **Assembled PEEK and acrylic microstructured reactors.**

min residence time. A 10 μL/min chalcone flow was pumped to the third inlet and mixed with the combined stream in the second staggered herringbone mixer. The resulting reaction mixture flowed to a 0.32 mL delay loop with a total residence time of 16 min, resulting in the base case reactant concentrations at the inlet of the epoxidation reactor of 13.47 g/L PLL, 0.132 mol/L peroxide, 0.0802 mol/L chalcone, 0.22 mol/L DBU. The reactor was maintained at the desired temperature by placing it in a water bath. The reaction was quenched at the reactor outlet by collecting the outlet flow in a stirred vial containing sodium sulfite. Clogging was found to occur and in initial scouting work, the reactors lasted only for several runs before clogging. To alleviate this, the reactors were flushed with the solvent (THF/ACN) before and after running the reactions. This was to prevent contacting the reactants dissolved in organic solvent with water, which may cause solids to precipitate due to insolubility of the reactants in water. While PEEK is chemically compatible with THF, some swelling of PEEK may occur if it is in contact with THF for prolonged periods. After each run, the reactors were flushed with the solvent followed by water to minimise contact with THF. Product analysis was performed by chiral HPLC and peroxide concentration was determined using the procedure of Gonsalves et al.,[15] as described in previous work.[6]

(14) Song, Y. J.; Kumar, C. S. S. R.; Hormes, J. *J. Micromech. Microeng.* **2004**, *14*, 932.

(15) Gonsalves, A. M. D. R.; Johnstone, R. A. W.; Pereira, M. M.; Shaw, J. *J. Chem. Res., Synop.* **1991**, 208.

Table 3. **Comparison of base case chalcone epoxidation in PEEK reactor at 23.1 °C and 16 min residence time with other reactors/models under similar operating conditions**

	conversion (%)	enantioselectivity to (2*R*,3*S*)-epoxide (%)
PEEK reactor	86.7	87.6
slit flow reactor model	89.6	92.4
continuous tubular reactor	88.4	88.8
continuous tubular model	88.3	92.4

Results and Discussion

Base Case. The base case conditions in the PEEK reactor at 23.1 °C resulted in an average conversion of 86.7% and an enantioselectivity value of 87.6%, as shown in Table 3. This compares well with the values predicted using the slit laminar flow reactor model, as well as with experimental results obtained using a continuous tubular reactor system[6] at the same reaction conditions. The experimental conversion values were within 3% from predicted values. The predicted enantioselectivity for both continuous experiments were larger than experimental values, although the experimental values were still within 5% of the predicted ones. Blank runs were carried out to determine if there are any other effects that could catalyse peroxide decomposition in the reactor. A solution of 0.53 mol/L peroxide and 53.88 g/L PLL was prepared and used. DBU was not added as it is known to catalyse the decomposition of the peroxide. Both inlet and outlet peroxide concentrations were determined to be at around 0.5 mol/L, indicating the absence of any other agents that could significantly catalyse peroxide decomposition.

Effect of Temperature. The effect of temperature, in the range 15−35 °C on the performance of a similar system in pure THF has previously been reported.[16] The rate of reaction at 35 °C was found to be 64% higher than that at 15 °C. In this work, reaction performance was investigated at three different temperatures, 15, 23.1 (base case) and 30 °C. It is expected that lower temperature may improve enantioselectivity, as it may slow down the background reaction compared to the catalysed reaction. However, lower temperature is also expected to result in lower overall reaction rate. Increasing reaction temperature is expected to increase overall reaction rate; however, as the temperature is increased beyond a specific value, the ratio of rate of background reaction to catalysed reaction rate is expected to increase, since the poly-L-leucine catalyst can be denatured at high temperatures. This will have the effect of lowering enantioselectivity at higher temperatures. The effect of temperature on PEEK reactor performance is shown in Figure 3. Conversion remained fairly constant as the temperature was raised from 15 to 23.1 °C, increasing slightly from 85.7 to 86.7% but decreased to 77% when the temperature was raised to 30 °C. Similarly, the enantioselectivity remained fairly constant up to 23.1 °C at around 87.6% but dropped to 84.5% when the temperature was raised to 30 °C. This is in contrast to the performance achieved in a continuous tubular reactor system, where the conversion increased from 88.4 to 94.6%, while the enantioselectivity remained fairly constant at around 89% when the temperature was increased from 23.1 to 30 °C.

(16) Carrea, G.; Colonna, S.; Meek, A. D.; Ottolina, G.; Roberts, S. M. *Tetrahedron: Asymmetry* **2004**, *15*, 2945. Carrea, G.; Colonna, S.; Meek, A. D.; Ottolina, G.; Roberts, S. M. *Chem. Commun.* **2004**, *12*, 1412.

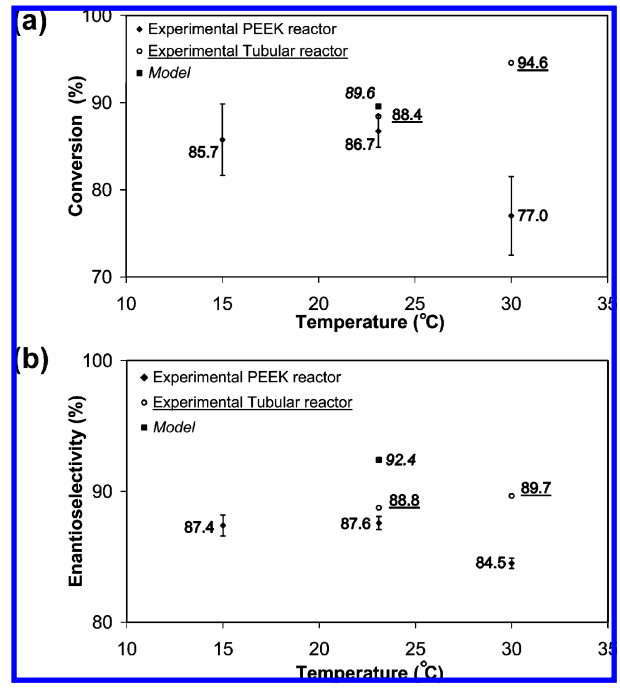

Figure 3. **(a) Effect of temperature on reaction conversion. (b) Effect of temperature on reaction enantioselectivity.**

These results suggest that at 30 °C, something seems to be happening in the PEEK reactor which causes the performance to deteriorate. It was visually observed during the experiments that, at higher temperatures, the outlet stream contained more bubbles than at lower temperatures. These bubbles are believed to form from the decomposition of peroxy anion, which is accelerated at higher temperatures. It is possible that these bubbles may cause formation of gas plugs within the reactor. Unlike tubular reactors, where the gas plugs are pushed along to the exit, the thin slits may cause the gas plugs to stagnate within the reactor, creating dead volumes, and hence shorter residence time results in lower conversion values.

Effect of Chalcone Concentration. The effect of chalcone concentration on both conversion and enantioselectivity was examined, keeping the concentrations of all other reactants at base case conditions, and the results are shown in Figure 4. The predicted values are also shown in dashed lines. The conversion gradually decreased from 87.9 to 64.5% as the chalcone concentration was increased from 0.0401 to 0.1604 mol/L, displaying the same trend predicted by the model. However, unlike the model, the conversion decreased only very slightly from a chalcone concentration of 0.0401 to 0.0802 mol/L. The enantioselectivity on the other hand, gradually increased from 82.5 to 88.0% as the chalcone concentration was increased, while the model predicted a somewhat constant enantioselectivity. The higher predicted conversion values at all chalcone concentrations is likely due to higher catalytic activity in the batch of catalyst used to determine the rate equations, as catalytic activity was observed to differ slightly from batch to batch. The predicted enantioselectivity on the other hand, was observed to display a different trend to that obtained experimentally. The values of enantioselectivity are primarily determined by the relative rates of catalysed and background reactions. The higher predicted values of enantioselectivity at all chalcone concentrations can similarly be attributed to a

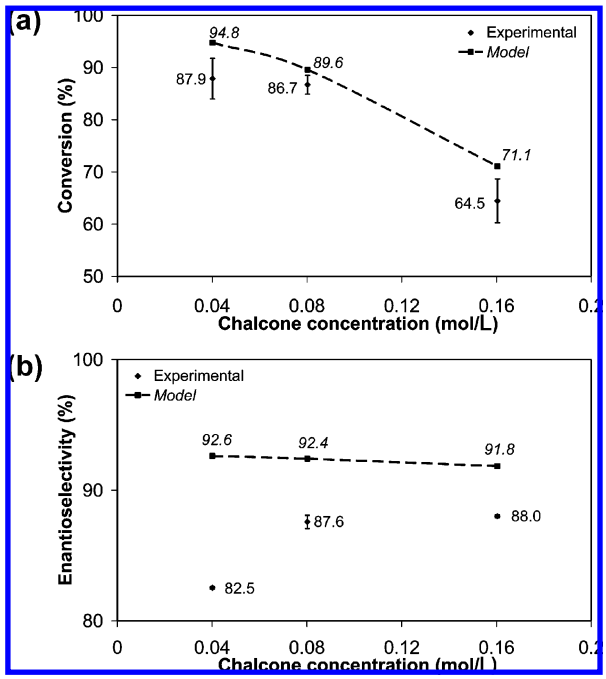

Figure 4. **(a) Effect of chalcone concentration on conversion in PEEK reactor. (b) Effect of chalcone concentration on enantioselectivity in PEEK reactor.**

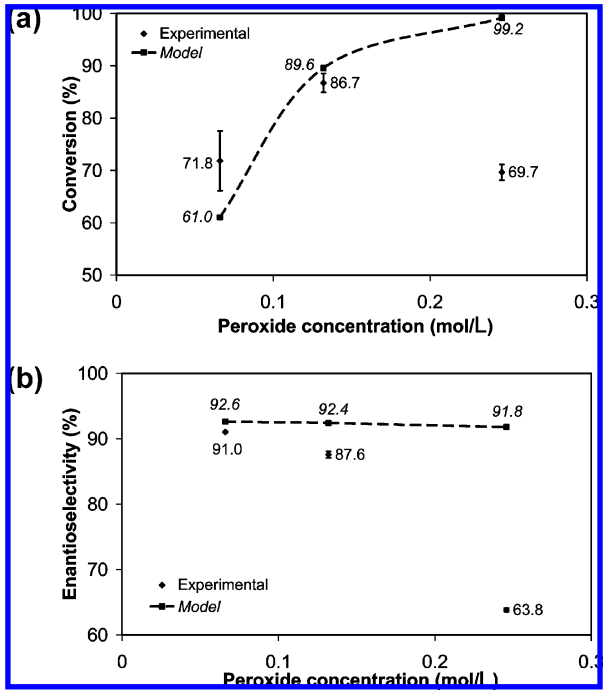

Figure 5. **(a) Effect of peroxide concentration on conversion in PEEK reactor. (b) Effect of peroxide concentration on enantioselectivity in PEEK reactor.**

difference in catalytic activity since a higher catalytic activity (in the batch used to determine the rate equations) would improve enantioselectivity. The difference between the predicted trend in enantioselectivity compared to the experimentally observed trend may be due to the fact that the rate equation for the background reaction was obtained in the absence of the catalyst, while in the presence of the catalyst this reaction is slowed down considerably, possibly due to the lack of free perhydroxyl ions, consistent with the view that the perhydroxyl ions are sequestered by the poly-L-leucine catalyst.[17]

Effect of Peroxide Concentration. The effect of peroxide concentration on the catalysed reaction was investigated at two conditions in addition to base case experiments, one at half and the other at nearly double the base case peroxide concentrations; the results are shown in Figure 5. The conversion increased from 71.8 to 86.7% and then decreased to 69.7% as the peroxide concentration was increased from 0.066 to 0.246 mol/L, in contrast with a predicted increase with increasing peroxide concentration. The enantioselectivity, on the other hand, showed a slight decrease from 91 to 87.6% and then decreased sharply to 63.8% at 0.246 mol/L, in contrast with the predicted slower decrease. The deviation from expected performance may be explained by the fact that the reactive species is not the peroxide itself but rather the perhydroxyl ion (OOH^-), and the change in reactive species concentration with a change in peroxide concentration was not captured by the model. The concentration of the reactive species at the start of the reaction is dependent on the concentrations of both the peroxide and DBU, as well as the residence time in the deprotonation reactor. The deprotonation of peroxide increases the concentration of the reactive species, while the base-catalysed decomposition of peroxide decreases the concentration of the reactive species. The base-catalysed decomposition of peroxide is given by:[18]

$$H_2O_2 + OOH^- \rightarrow H_2O + OH^- + O_2$$

and the corresponding rate equation is of type:

$$\text{Rate}_{\text{decomposition}} = k[H_2O_2][OOH^-] \qquad (20)$$

These factors suggest an optimum condition may exist, where the concentration of the reactive species is maximised. An estimate of the equilibrium perhydroxyl ion concentration for all three experimental conditions is shown in Table 4.[19] The deprotonation was assumed to be instantaneous; however, as actual data on the rate of deprotonation were not available, the equilibrium perhydroxyl ion concentration represents the maximum expected concentration, with actual perhydroxyl ion concentration possibly lower than this value. Several different reactant concentration ratios are also provided in Table 4 to aid analysis of the experimental results. At peroxide concentration of 0.066 mol/L, the equilibrium perhydroxyl concentration was found to be 0.0555 mol/L and equivalent to around 0.7 of the chalcone concentration. The conversion was therefore limited to around 71.8% by the available perhydroxyl ion concentration. The conversion value predicted by the model, however, was much lower at 61%. At peroxide concentration of 0.246 mol/L, a sharp drop in conversion to 69.7% was observed in contrast to the predicted increase in conversion to 99.2%. This may be related to the fraction of perhydroxyl ions formed from hydrogen peroxide (fourth column, Table 4) which was lower than that implied by the model. Other possible

(17) Lopez-Pedrosa, J. M.; Pitts, M. R.; Roberts, S. M.; Saminathan, S.; Whittall, J. *Tetrahedron Lett.* **2004**, *45*, 5073.
(18) Evans, D. F.; Upton, M. W. *J. Chem. Soc., Dalton Trans.* **1985**, 2525.
(19) Kee, S. P. Microreactor Engineering Studies for Asymmetric Chalcone Epoxidation. PhD Thesis. University College London, 2007.

Table 4. **Equilibrium perhydroxyl ion concentration at different peroxide concentrations**

$[H_2O_2]$ (mol/L)	$[DBU]/[H_2O_2]$	$[OOH^-]$ (mol/L)	$[OOH^-]/[H_2O_2]$	$[OOH^-]$/[Chalcone]	[PLL]/$[OOH^-]$ g/mol
0.066	3.33	0.0555	0.841	0.69	243
0.132	1.67	0.0933	0.707	1.16	144
0.246	0.90	0.1326	0.54	1.65	102

Table 5. **Equilibrium perhydroxyl ion concentrations at different DBU concentrations**

[DBU] (mol/L)	$[DBU]/[H_2O_2]$	$[OOH^-]$ (mol/L)	$[OOH^-]/[H_2O_2]$	$[OOH^-]$/[Chalcone]	[PLL]/$[OOH^-]$ g/mol
0.11	0.83	0.0685	0.519	0.85	197
0.22	1.67	0.0933	0.707	1.16	144
0.44	3.33	0.111	0.841	1.38	121

explanations for the drop in conversion at 0.246 mol/L peroxide concentration include incomplete deprotonation (longer time required to reach equilibrium concentration) and the base-catalysed decomposition of peroxide[18] which increases with increasing perhydroxyl ion concentration as shown in eq 20 and may result in increased formation of oxygen bubbles which can reduce the residence time in the reactor.

Both predicted and experimental enantioselectivity values decrease with increasing peroxide concentration, although the predicted values are higher than the experimental values in all cases. The higher enantioselectivity at all peroxide concentrations can be explained in part by the higher catalytic activity of the catalyst batch used for the kinetic studies. The big decrease in experimental enantioselectivity at peroxide concentration of 0.246 mol/L, may be due to the increased availability of free peroxide, because of the lower ratio of catalyst concentration to perhydroxyl ion concentration. The higher rate of background reaction to rate of catalysed reaction may imply that substrate saturation of the catalyst has been reached, and therefore, any further increase in peroxide concentration would only increase the background reaction. The discrepancy between experimental and predicted results can also be attributed to the fact that this concentration falls outside the range of the concentration for the kinetic studies (which was limited to a maximum peroxide concentration value of 0.14 mol/L).

Effect of DBU Concentration. The effect of DBU concentration on the performance of the catalysed reaction was also examined at two additional DBU concentrations. The DBU concentration was expected to affect the reaction performance in a manner similar to that of the peroxide concentration, as they both influence the concentration of the reactive species. The estimated equilibrium concentrations of perhydroxyl ion at all three DBU concentrations are shown in Table 5. The changes in conversion and enantioselectivity with a change in DBU concentration are shown in Figure 6. At DBU concentration of 0.11 mol/L, conversion was only 45.1%, even though the estimated equilibrium perhydroxyl ion concentration was 0.85 times the chalcone concentration. In comparison, a conversion of 71.8% was achieved when the equilibrium perhydroxyl ion concentration was 0.69 times the chalcone concentration (see Table 4). In both cases, the reduction in either DBU or peroxide concentration resulted in a limiting equilibrium perhydroxyl ion concentration, yet in the latter case the conversion achieved was much higher. At lower DBU concentration of 0.11 mol/L, the lower conversion of 45.1% was not due to a limiting equilibrium perhydroxyl ion concentration but possibly to a lower rate of deprotonation, resulting in lower concentration of the reactive species. The lower enantioselectivity of 74.7% compared to base case could also be explained by a slower rate of deprotonation, which would lead to fewer perhydroxyl ions sequestered by the poly-L-leucine catalyst by the time the catalyst/peroxide mixture enters the epoxidation stage. As the DBU concentration is increased to 0.22 mol/L, both conversion and enantioselectivity increased to 86.7 and 87.6%, respectively. Both of these can be attributed to faster deprotonation rate as discussed. As the DBU concentration was increased to 0.44 mol/L, the conversion remained approximately constant, while enantioselectivity was reduced to 82.7%, indicating enhancement of the background reaction.

Effect of Catalyst Concentration. The effect of catalyst concentration was examined at two other catalyst concentrations in addition to the base case concentration, and the results are shown in Figure 7. The conversion increased from 51.5 to 86.7%, displaying a trend similar to that of predicted values when the catalyst concentration was increased from 6.74 to 13.47 g/L. On increasing the catalyst concentration further to 20.21 g/L, the conversion decreased to 75.8% in contrast to a predicted increase to 95.5%. Similarly, the enantioselectivity values increased from 71.4% to 87.6% but then decreased to

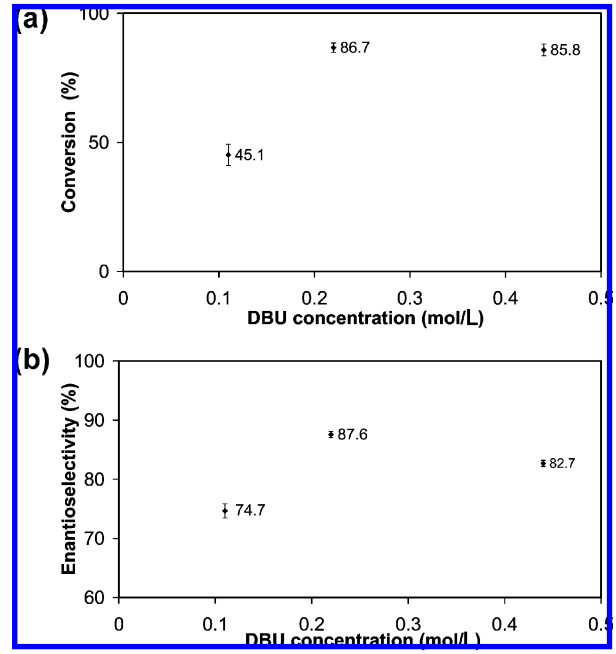

Figure 6. **(a) Effect of DBU concentration on conversion in PEEK reactor. (a) Effect of DBU concentration on enantioselectivity in PEEK reactor.**

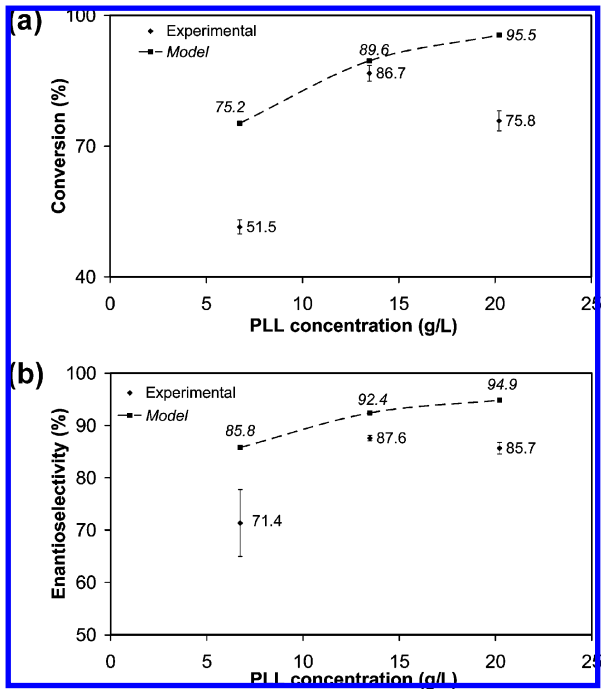

Figure 7. **(a) Effect of PLL concentration on conversion in PEEK reactor. (b) Effect of PLL concentration on enantioselectivity in PEEK reactor.**

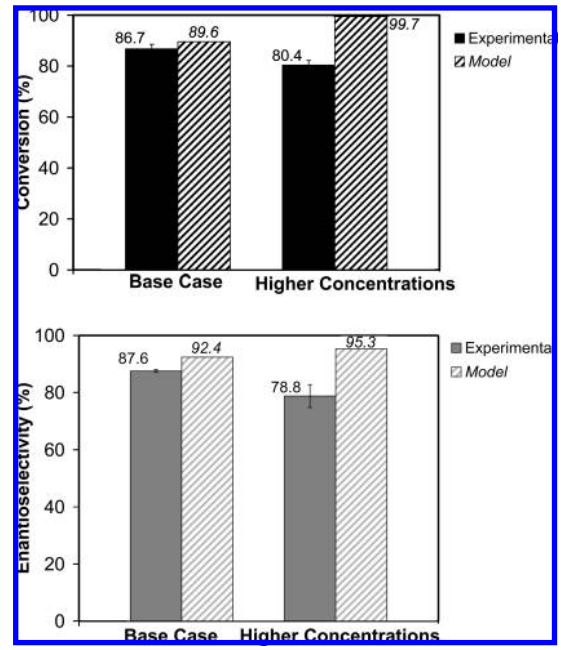

Figure 8. **(a) Effect of higher concentrations of all reactants on conversion. (b) Effect of higher concentrations of all reactants on enantioselectivity.**

85.7%, in contrast to model prediction. The reductions in both conversion and enantioselectivity values with a decrease in catalyst concentration are in line with expectations, since the relative rate of the catalysed to background reaction rate will decrease due the slowing of the catalysed reaction rate. The conversion and enantioselectivity values predicted by the model at 6.74 g/L catalyst concentration were much higher than the experimental values. It must be noted that the catalyst concentration of 6.74 g/L does not fall within the catalyst concentration range used in the kinetic studies. The decrease in experimental conversion and enantioselectivity values at the catalyst concentration of 20.21 g/L in contrast to model prediction may be due to incomplete mixing, induced by a decrease in molecular diffusivity and an increase in viscosity of the reaction mixture. As the catalyst concentration was increased, the catalyst solution became more viscous. For an epoxidation-stage catalyst concentration of 20.21 g/L, the corresponding catalyst concentration in the deprotonation stage would be 40.42 g/L.

Given the average density of the THF/ACN solvent is 837.73 kg/m^3, the weight fraction of the catalyst in the solution is about 0.05 and hence can be classified as a dilute polymeric solution.[20] In general, solutions of proteins are not treated as polymeric solutions; however, the catalyst in this case is tethered on polyethylene glycol with a much larger molecular weight (the molecular weight of polyethylene glycol with 82 monomers ≈ 5084 compared to the molecular weight of 15 monomers of L-leucine of 1965) and hence can be treated as a dilute polymeric solution. Thus, as the catalyst concentration is increased, the diffusivity is decreased, although in general this decrease in diffusivity is not expected to be as large as the increase in relative viscosity.[21] This decrease in diffusivity could affect the conversion by reducing the rate at which the reactants come into contact. The lower enantioselectivity value could be explained by the slower diffusivity; however, the higher catalyst/perhydroxyl ion concentration ratio should compensate for this effect. Since the viscosity of a solution usually increases drastically when a small amount of polymer is dissolved in it,[21] the poor performance at high catalyst concentration is more likely due to incomplete mixing caused by the increased viscosity. A high viscosity ratio between the two mixing fluids can cause a deviation in velocity profile from Poiseuille flow. Using micro-Particle Image Velocimetry (PIV) measurements of two-fluid flow in a Y-shape microchannel at high viscosity ratios, the high viscosity fluid was found to occupy a larger portion of the cross-sectional area.[22] The high viscosity ratio is likely to also affect the velocity profile and mixing behaviour in the staggered herringbone mixer.

Higher Concentrations of All Reactants. In an effort to increase the rate of production, the effect of increasing the concentrations of all reagents by the same factor (×1.85) was investigated. As shown in Figure 8, conversion decreased from 86.7 to 80.4% in contrast to a predicted increase from 89.6 to 99.7%. Enantioselectivity decreased from 87.6 to 78.8% compared to a predicted increase from 92.4 to 95.3%. The difference between experimental and predicted results can be similarly explained by incomplete mixing due to the lowering of solute diffusivities and increase in viscosity of reaction mixture with an increase in the catalyst concentration. However, while the catalyst concentration was even higher at 25.03 g/L in this case, (compared to 20.21 g/L in the previous section), the conversion obtained was higher than that obtained previously (75.8%), while the enantioselectivity obtained was lower than the 85.7% achieved previously. The following explanation may

(20) Cussler, E. L. *Diffusion: Mass Transfer in Fluid Systems*, 2nd ed.; Cambridge University Press: Cambridge, 1997.

(21) Li, S. U.; Gainer, J. L. *Ind. Eng. Chem. Fundam.* **1968**, *7*, 433.
(22) Kim, B. J.; Liu, Y. Z.; Sung, H. J. *Meas. Sci. Technol.* **2004**, *15*, 1097.

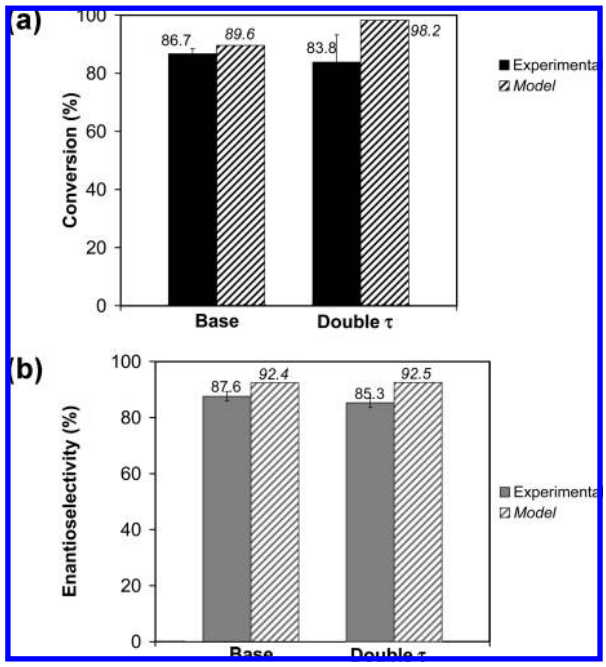

Figure 9. **(a) Effect of longer residence time on conversion. (b) Effect of longer residence time on enantioselectivity.**

be offered for this behaviour. In both cases, the solution viscosities would have increased while the solute diffusivities would have decreased, although at 25.03 g/L catalyst, the viscosity is expected to be higher, and diffusivity is expected to be lower than that at 20.21 g/L. The conversion in this case is higher because, unlike the case in the previous section, the concentrations of all other reactants were also doubled, and hence a higher overall reaction rate was achieved. As with the previous case, the higher viscosity and possibly lower diffusivity resulted in incomplete mixing increasing the free perhydroxyl ion concentration available for the background reaction.

Effect of Residence Time. The reaction performance was investigated at double the base case residence time by halving the reactant flow rates. Doubling of the residence time resulted in a decrease in conversion from 86.7 to 83.8% in contrast to a predicted increase, while the enantioselectivity decreased slightly from 87.6 to 85.3%, as shown in Figure 9. It is interesting to note that the results were consistent with the results obtained from a batch experimental study of the effect of deprotonation time, where the conversion decreased slightly (∼4%), while the enantioselectivity remained approximately constant, as the deprotonation time was increased. The reaction did not proceed to near completion as predicted, even with the doubling of the residence time, because the reactive species is not the peroxide but the perhydroxyl ion, whose concentration is determined by the rate of deprotonation and the rate of decomposition of the perhydroxyl ion as well as the residence time in the deprotonation reactor. With doubling of the residence time in both deprotonation and epoxidation reactors, the lower conversion is probably due to the effect of decomposition of the perhydroxyl ions. The experimental performance is expected to more closely match values predicted by the model if the residence time in the deprotonation reactor is maintained at 30 min while doubling the residence time in the epoxidation reactor.

Concluding Remarks

The design of a microstructured reaction system for poly-L-leucine-catalysed asymmetric epoxidation of chalcone was performed, aided by a mathematical reactor model using reaction rate equations established independently. An integrated planar format was adopted, so that the reactor system would be amenable to scale out. Staggered herringbone mixers were selected to enhance mixing, as they allow rapid mixing with high throughput and lower pressure drop as compared to a plain T-mixer. The reactor channel was dimensioned accordingly to maximise the effects of diffusion so that it approximates a plug flow reactor. Reaction heat effects were not found to be important. The reactor was fabricated in PEEK spin-coated with SU-8, due to its high chemical resistance and low cost of fabrication. Fouling of the reactors was alleviated by using inline filters and establishing suitable operating procedures. The reaction at base case conditions achieved a conversion of 86.7% and an enantioselectivity of 87.6%, in good agreement with values predicted by the model. A parametric study of the effects of reaction temperature, residence time, and concentrations of the various reactants and catalyst on the reaction performance was carried out. The results of the parametric study and their comparison to the model demonstrated the complexity of the system and the many factors which influence its performance. The system is essentially a two-step reaction with the concentration of the free perhydroxyl ions influenced by the outcome of the deprotonation step. Methods to optimise the reaction conditions must therefore take into account the effects of varying parameters on the deprotonation reaction, since this affects the initial concentration of the perhydroxyl ion. Some of the parameters which can influence the deprotonation include DBU concentration, temperature, and deprotonation residence time. The results also suggest that base-catalysed decomposition of perhydroxyl ions reduces the concentration of the reactive species, with corresponding formation of bubbles that may stagnate in the rectangular cross-section reaction channels. The reaction system considered in the kinetic study[5] was sufficient for simple design purposes but may not have captured the full underlying chemistry. For example, erosion of enantioselectivity was assumed to occur only by the background reaction, and perhydroxyl ion concentrations were not considered directly in the kinetic equations. There appears to be a maximum catalyst concentration beyond which performance is not further improved in this reactor; this was attributed to the fact that an increase in catalyst concentration resulted in a corresponding increase in viscosity and decrease in diffusivity values, both of which influence mixing performance. The use of concentrated reactants to speed up the reaction resulted in poorer performance and increased the likelihood of fouling. This study demonstrates that in addition to suitable kinetic information, other phenomena need to be considered for optimising the performance of continuous microchannel reactors.

Acknowledgment

Financial support from the Foresight LINK programme is gratefully acknowledged. We also thank Philip Summersgill from Epigem for help in reactor fabrication.

NOMENCLATURE

C_n	Concentration of component n, mol/L
C_p	Specific heat capacity, kJ/kg·K
d	Diameter, m
D	Diffusion coefficient, m^2/s
D_E	Equivalent diameter, m
h	Channel height, m
H_{Rxn}	Heat of reaction, kJ/mol
k	Rate constant, $L^2/g \cdot mol \cdot s$
k_{BG}	Background reaction rate constant, L/mol·s
$K_{Chalcone}$	Equilibrium constant associated with chalcone, L/mol
$K_{H_2O_2}$	Equilibrium constant associated with hydrogen peroxide, L/mol
L	Length, m
Pe_r	Radial Péclet number, -
Pe_z	Axial Péclet number, -
Q	Volumetric flow, m^3/s
$\mathscr{R}_n$	Change in component n concentration due to reaction, mol/L·s
Re_d	Reynolds number based on channel diameter, -
S	Enantioselectivity, -
Sc	Schmidt number, -
t	time, s
T	Temperature, K
T_{wall}	Wall temperature, K
u	Velocity, m/s
$\bar{u}$	Average velocity, m/s
V_z	Axial velocity profile, m/s
w	Channel width, m
X	Conversion, -
y	Transverse coordinate, -
Y	Half of slit height, m
z	Axial coordinate, -
[Cat]	Catalyst loading, g/L
[Chalcone]	Chalcone concentration, mol/L
$[H_2O_2]$	Hydrogen peroxide concentration, mol/L

GREEK LETTERS

α	Mixer parameter. Ratio of groove half-height to channel height, -
α_T	Thermal diffusivity, m^2/s
ΔP	Pressure drop, Pa
ζ	Dimensionless transverse coordinate, -
λ	Thermal conductivity, W/m·K
μ	Viscosity, Pa·s
ξ	Dimensionless axial coordinate, -
ρ	Density, kg/m^3
τ	Residence time, s

SUBSCRIPTS

0	Initial conditions
n	Component
mix	Mixing cup average
dif	Diffusional

Received for review October 27, 2008.

OP800276A